Model for the electron distribution in modulation-doped heterostructures with high density of surface states

Rolf R. Gerhardts
Max-Planck-Institut für Festkörperforschung, Heisenbergstrasse 1, D-70569 Stuttgart, Germany
(Received 29 March 2010; revised manuscript received 4 May 2010; published 28 May 2010)

We study heterostructures, consisting of parallel layers of GaAs and $Al_xGa_{1-x}As$ containing n-doped sheets and, on both sides, GaAs cap layers with a high density of surface states. Assuming thermal equilibrium between the electrons in the surface states, the donor-induced states, and the eigenstates near the $GaAs/Al_xGa_{1-x}As$ interface (IF), we obtain three different doping regimes. At low doping only the surfaces are charged with electrons, not the IF. At intermediate doping also a two-dimensional electron system (2DES) near the IF occurs. At high doping the electron densities of the surface layers and of the 2DES saturate, and a parallel channel occurs at the highly doped sheet, which accommodates the electrons resulting from further doping. Besides the results of a self-consistent Hartree-type calculation we present a quasiclassical approach, which gives very good results for the electron distribution over the sample in all three doping regimes. In the heavy-doping saturation regime also a simple electrostatic estimate is applicable.

DOI: 10.1103/PhysRevB.81.205324 PACS number(s): 73.20.−r, 73.21.Ac

I. INTRODUCTION

The basic idea of modulation-doping[1,2] is, to increase the mobility of a two-dimensional electron system (2DES) in a heterostructure by a spatial separation of the 2DES from the ionized donors, which provide the electrons. This reduces the scattering of the electrons by the randomly distributed donor ions and, thereby, increases the mobility of the 2DES. Modulation-doping has proven to be a very effective tool to achieve in GaAs based heterostructures 2DESs with very high mobility at low temperatures, where phonon scattering becomes unimportant. This is of extreme importance for the investigation of several new effects, which have recently been detected on single and double quantum well structures submitted to strong magnetic fields, e.g., the occurrence of fractional quantum Hall states with half-integer filling fraction[3,4] or of an intrinsic spin lattice.[5]

One expects that the low-temperature mobility increases with the spacer thickness, provided the volume density of background impurities can be made sufficiently small. Recently mobilities of 2DESs in δ-doped GaAs-based heterostructures have been calculated[6] for different electron densities n, spacer thicknesses d, and two-dimensional (2D) donor densities n_d. Mobilities as large as 10^8 $cm^2/V\,s$ have been predicted[6] at $T=1$ K, $n=3\times10^{11}$ cm^{-2} for $d=120$ nm and $n_d=10^{11}$ cm^{-2}. Here n, d, and n_d are considered as independent parameters, which can be chosen arbitrarily. This may be true within certain limits for gated heterostructures, but it is certainly not true for the frequently investigated ungated structures.

In ungated Si-doped $GaAs/Al_xGa_{1-x}As$ heterostructures the electron density n cannot be larger than the donor density n_d, and in real samples n is usually much smaller than n_d. The reason is that such structures are usually fabricated with GaAs cap layers, which are known to accommodate a large density of surface states with energies deep in the fundamental gap.[7,8] For weak doping, the electrons provided by the donors occupy such surface states and fix the Fermi energy into this energy region. With increasing doping the electrostatic dipole potentials, produced by a negative surface charge and a positively charged doping layer, lower the conduction-band inside the heterostructure toward the Fermi energy, so that eventually bound states near an internal interface can be occupied and a 2DES occurs.

The purpose of the present paper is to incorporate well-known facts about the electronic surface states[8] into a quantitative model, which allows calculating, as function of the doping level, the electron density in the 2DES and on the surfaces. For very high doping this model yields, in addition to the desired 2DES and in agreement with many experimental observations, a parallel channel (PC) located immediately at the high-doping region. The electrons in this PC interact strongly with the nearby charged donor ions, and consequently have a low mobility. Due to screening and correlation effects, they may modify the effective scattering potential experienced by the electrons of the desired 2DES, and thus strongly affect its mobility.[9] Experimentally it is usually impossible to contact the desired 2DES and the PC separately, and it is difficult to get information about electron density and transport properties of both, the desired 2DES and the PC. If, however, the 2DES exhibits the quantum Hall effect and several plateaus at integer filling factors can be investigated, such information can be obtained.[10]

The scope of this paper is as follows. In Sec. II, the model is explained for the case of a quantum well structure, and the results from self-consistent, Hartree-type calculations for the distribution of charges over the structure are presented. In Sec. III, a quasiclassical approximation for the distribution of areal charges is developed, which neglects the vertical extent of 2DESs so that the potential becomes piecewise linear. Moreover, binding energies are replaced by simple estimates, which allows to establish sets of linear equations for the charge densities in the three different doping regimes. In Sec. IV, the quantum well is replaced by a single interface, and two cases are considered, one with an electrostatic field in the GaAs layer, which supports binding of a 2DES to the interface, and another case without such a field. In the latter case, with increasing doping a second subband will be occu-

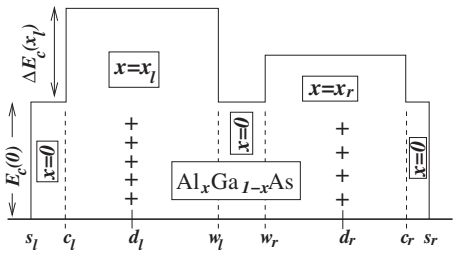

FIG. 1. Sketch (not to scale) of the conduction-band edge (without charge-induced band bending) of the $Al_xGa_{1-x}As/GaAs$ heterostructure with pure GaAs ($x=0$) in $w_l<z<w_r$ (the well) and in $s_l<z<c_l$ and $c_r<z<s_r$ (the caps). For the quantum-well structure we take $x_l=x_r\sim 0.3$, for the single-interface heterostructure $x_l\sim 0.3$ and $x_r=0$. Si doping is confined to the sheets at $z=d_l$ and $z=d_r$.

pied in the desired 2DES, long before a parallel channel occurs at the doping sheet. The most important results are summarized in Sec. V, and it is emphasized that the heavy-doping limit, in which the electron density of the desired 2DES saturates, is easily understood by simple electrostatic arguments.

II. BASICS ON MODEL AND APPROACH

We consider a simple model of a heterostructure, which is flexible enough to describe, according to the choice of parameters, either a quantum well structure or a structure with a single inner $Al_xGa_{1-x}As/GaAs$ interface at which a 2DES can occur. The shape of the structure is sketched in Fig. 1. It is terminated by GaAs cap-layers located at $s_l<z<c_l$ and $c_r<z<s_r$. We will first consider a quantum well structure by choosing $x_r=x_l\sim 0.3$, and later a single-interface structure by choosing $x_l\sim 0.3$ and $x_r=0$. We allow for surface charges at $z=s_l$ and $z=s_r$ and for positively charged planes at $z=d_l$ and $z=d_r$ describing the effect of δ-doping. We assume Si-doping and are aware of the fact that for Al-concentration $0.2\leq x\leq 0.4$, only a fraction of the Si atoms will lead to shallow donors, which are completely ionized, while the rest leads to deep donors, which, without appropriate photoexcitation at low temperature, may be only partly ionized.[11] We consider only the ionized donors, neglect possible charge-correlation effects, which may affect the mobility of the 2DES,[9] and assume that the ionized donors are homogeneously distributed over the sheets at d_l and d_r with area densities n_{Dl} and n_{Dr}, respectively.

The material parameters are taken from the literature,[12–14] i.e., for $x\lesssim 0.3$ the fundamental band gap is $E_g(x)=(1.518+1.30x+0.312x^2)$ eV, and for the difference between the conduction band edges of $Al_xGa_{1-x}As$ and GaAs we take $\Delta E_c(x)=0.69[E_g(x)-E_g(0)]$. The dielectric constant and the effective conduction band mass are chosen as $\varepsilon(x)=12.4-2.34x$ and $m^\star(x)=(0.0665+0.0835x)m_0$, respectively, with m_0 as the free-electron mass.

The properties of surface states are discussed in Ref. 8. Low-energy valence-band-like states are separated from conduction-band-like states at higher energies by the charge neutrality level $E_{\rm cnl}$. The density of surface states near $E_{\rm cnl}$ is

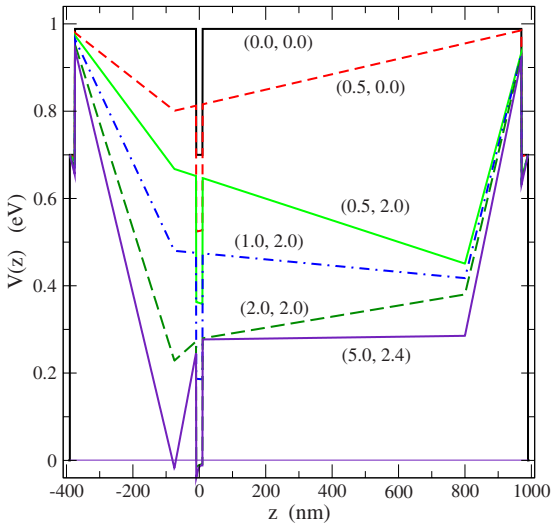

FIG. 2. (Color online) Effective conduction-band edge $V(z)$ for a QW structure between $s_l=-390$ nm and $s_r=990$ nm, with GaAs cap layers at $z<-375$ nm and $z>970$ nm, and a GaAs well at $|z|<w_r=-w_l=10$ nm. The Al-concentration in the other layers is $x_l=x_r=0.3$. Positive charges of area density $e\nu_l\times 10^{11}$ cm^{-2} at $d_l=-75$ nm and $e\nu_r\times 10^{11}$ cm^{-2} at $d_r=800$ nm describe the effect of δ-doping and are indicated by the labels (ν_l,ν_r) at the graphs.

taken as $D_S\approx 4\times 10^{14}/(\text{eV cm}^2)$ so that a Fermi energy E_F will lead to a surface charge density $-eD_S(E_F-E_{\rm cnl})$. From Ref. 8 one obtains $E_c-E_{\rm cnl}\approx 1$ eV, but we will also consider $E_c-E_{\rm cnl}=0.7$ eV to be consistent with the widely reported midgap pinning of the Fermi energy as a consequence of surface states.

We will take the charge neutrality level at the left surface ($z=s_l$) as energy zero, so that in the absence of free charges the position dependent conduction band edge is $V_{cb}(z)=E_c(0)+\Delta E_c[x(z)]$, where $x(z)$ is the Al concentration at z (see Fig. 1). For a simple quantum well (QW) structure with $x_l=x_r=0.3$ this is shown by the uppermost curve in Fig. 2, labeled (0.0,0.0). Doping introduces free charges into the structure and the resulting electrostatic potential adds to $V_{cb}(z)$ and leads to a band bending with the effective conduction band edge,

$$V(z)=V_{cb}(z)+V_C(z),\quad V_C(z)=V_{\rm fc}(z)+V_H(z),\qquad (1)$$

where $V_{\rm fc}(z)$ is produced by the fixed doping and surface charges, while $V_H(z)$ describes the effect of mobile electrons in the 2DES and, eventually, a parallel channel, which we treat in the Hartree approximation.

We will assume overall charge neutrality of the structure, so that the electric field $V_C'(z)/e$ vanishes for $z\leq s_l$ and for $z\geq s_r$, and we take the boundary condition $V_{\rm fc}(s_l)=V_H(s_l)=0$. Then the 2D electron densities are determined by

$$n_{Sl}=D_SE_F,\quad n_{Sr}=D_S[E_F-V_C(s_r)]\qquad (2)$$

for the left and right surface, respectively, and by the charge neutrality condition

$$n_{Sl} + n_{Sr} + n_{\rm el} = n_{Dl} + n_{Dr}, \tag{3}$$

with $n_{\rm el}$ the areal density of the 2DES in the QW. The potentials due to the charged planes are easily calculated,

$$V_{\rm fc}(s_r) = \frac{4\pi e^2}{\varepsilon(0)}[-d_{srsl}n_{Sl} + d_{srdl}n_{Dl} + d_{srdr}n_{Dr}], \tag{4}$$

where

$$d_{srdr} = q_r(c_r - d_r) + s_r - c_r,$$

$$d_{srdl} = q_l(w_l - d_l) + w_r - w_l + q_r(d_r - w_r) + d_{srdr},$$

$$d_{srsl} = c_l - s_l + q_l(d_l - c_l) + d_{srdl}, \tag{5}$$

with $q_l = \varepsilon(0)/\varepsilon(x_l)$ and $q_r = \varepsilon(0)/\varepsilon(x_r)$.

Equations (2)–(4) allow to calculate the surface electron densities n_{Sl} and n_{Sr} in terms of the areal densities of ionized donors, n_{Dl} and n_{Dr}, of mobile electrons $n_{\rm el} = n_{\rm mob}$, and of the Hartree potential $V_H(s_r)$ at the right surface,

$$n_{Sl} = [g_{srdl}n_{Dl} + g_{srdr}n_{Dr} - n_{\rm mob} + D_S V_H(s_r)]/Z_0, \tag{6}$$

and $n_{Sr} = n_{Dl} + n_{Dr} - n_{Sl} - n_{\rm mob}$, with $g_{srdl} = 1 + \gamma d_{srdl}$, $g_{srdr} = 1 + \gamma d_{srdr}$, etc., where $\gamma = 4\pi e^2 D_S/\varepsilon(0)$ and $Z_0 = 1 + g_{srsl}$.

A. Weak doping

Without doping, $n_{Dl} = n_{Dr} = 0$, there are no free charges in the structure, and the Fermi energy coincides with the charge neutrality level, $E_F = E_{\rm cnl} = 0$. The bottom of the well potential is at the conduction band edge of GaAs, $E_c(0)$ [we take $E_c(0) = 0.7$ eV], i.e., much higher than the Fermi level, see graph labeled (0.0,0.0) in Fig. 2. For weak doping the electrons from the donor levels, which are located slightly below the conduction band edge in the doping region, move to the surface states. The resulting negative surface charge increases the Fermi energy, but only slightly, because of the large surface density of states (DOS) D_S. As a consequence, for sufficiently weak doping, the well region remains free of electrons, $n_{\rm el} = 0$, and with $V_H(s_r) = 0$ Eq. (6) simplifies to a linear dependence of n_{Sl}, and consequently of n_{Sr}, on n_{Dl} and n_{Dr}. The four upper graphs in Fig. 2, labeled by (ν_l, ν_r), show the effective conduction band edge for zero and weak doping situations with $n_{Dl} = \nu_l \times 10^{11}$ cm^{-2} and $n_{Dr} = \nu_r \times 10^{11}$ cm^{-2}. The graphs labeled (2.0,2.0) and (5.0,2.4) represent the intermediate- and the heavy-doping situation to be discussed in the following.

B. Intermediate doping

The dipole potentials, due to the positively charged doping sheets and the negatively charged surfaces, lower $V(z)$ inside the structure, especially at the QW. If doping becomes so strong that the lowest energy eigenvalue in the QW becomes lower than E_F, this eigenstate will be occupied and a 2DES will occur in the QW. Now the electron volume-density $N_{\rm el}(z)$ and the Hartree potential $V_H(z)$ must be calculated self-consistently. To calculate $V_H(z)$, we integrate Poisson's equation

$$\frac{d}{dz}\varepsilon(x(z))\frac{d}{dz}V_H(z) = -4\pi e^2 N_{\rm el}(z), \tag{7}$$

with $V_H'(b) = 0$ and $V_H(b) = 0$ for a suitable position b with $N_{\rm el}(z) = 0$ for $z < b$. Solving the eigenvalue problem

$$\left\{-\frac{d}{dz}\frac{\hbar^2}{2m^\star[x(z)]}\frac{d}{dz} + V(z) - E_n\right\}\psi_n(z) = 0, \tag{8}$$

with the potential $V(z)$ of Eq. (1), we obtain in the low-temperature limit

$$N_{\rm el}(z) = D_0 \sum_n |\psi_n(z)|^2 (E_F - E_n)\,\theta(E_F - E_n), \tag{9}$$

with $D_0 = m^\star(0)/(\pi\hbar^2) = 2.79 \times 10^{10}/(\text{cm}^2\,\text{meV})$ the 2D conduction-band DOS of GaAs. Since the eigenfunctions $\psi_n(z)$ are normalized, the z integral over Eq. (9) yields

$$n_{\rm el} = D_0 \sum_n (E_F - E_n)\,\theta(E_F - E_n). \tag{10}$$

To solve the Hartree-Poisson problem for given doping n_{Dl} and n_{Dr}, we proceed as follows. First we choose a value for $n_{\rm el} (< n_{Dl} + n_{Dr})$ and guess a corresponding approximation for $V_H(s_r)$, e.g., $V_H^{(0)}(s_r) = -4\pi e^2 d_{srw0} n_{\rm el}/\varepsilon(0)$ with $d_{srw0} = w_r - w_0 + q_r(c_r - w_r) + s_r - c_r$, which would be the correct value if the 2DES would be confined to the plane $w_0 = (w_r + w_l)/2 = 0$. Inserting $n_{\rm el}$ and the starting value for $V_H(s_r)$ into Eq. (6), we obtain starting values for the surface electron densities n_{Sl} and n_{Sr}. The area densities n_{Sl} and n_{Dl} determine the potential $V_{\rm fc}(z)$ in the well region. For fixed external potential $V_{cb}(z) + V_{\rm fc}(z)$ we solve the Hartree-Poisson problem by weighted iteration, adding in each step a small fraction $\gamma_{\rm new} (\lesssim 0.1)$ of the new potential to a large fraction $\gamma_{\rm old} = 1 - \gamma_{\rm new}$ of the old one. After convergence we get a better approximation to $V_H(s_r)$. With this we repeat the process and iterate until the value of $V_H(s_r)$ does no longer change (by more than 10^{-4} meV). From the converged solution we get a Fermi energy $E_F^{2D} = E_1 + n_{\rm el}/D_0$ of the 2DES (provided only the lowest state in the QW is occupied), in addition to the surface Fermi energy $E_F^S = n_{Sl}(n_{\rm el})/D_S$. Now we change $n_{\rm el}$ until these two Fermi energies agree (up to 10^{-5} meV). If this agreement is achieved, we have the correct thermal equilibrium solution. Figure 3 shows the result of such a calculation for the QW structure sketched in Fig. 2.

C. Heavy doping

If we increase, in a structure like that of Fig. 3, the doping density n_{Dl} in the left doping sheet, the potential minimum at $d_l = -75$ nm becomes deeper, and localized quantum states occur in this minimum. If the lowest energy eigenvalue of these states, $E_1^{\rm pc} > V(d_l)$, falls below the Fermi energy, this state will become occupied and a second 2DES, a PC in addition to the desired 2DES, will occur in the doping region. For an equilibrium calculation we have to take this PC into account, and we will treat it on the same footing as the intended 2DES.

Such a treatment is certainly reasonable, if the donor density n_{Dl} is so large, that the shallow donor states in the plane

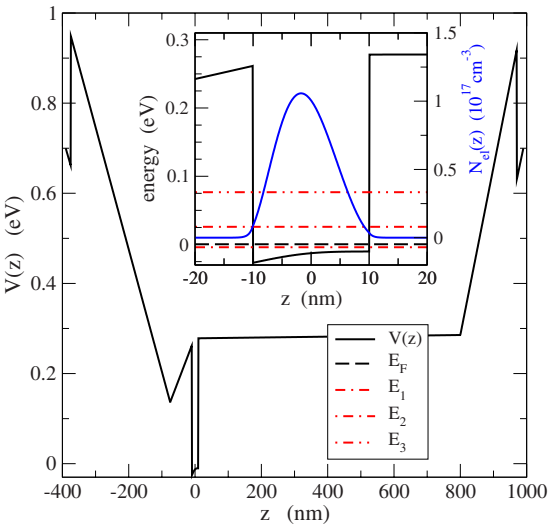

FIG. 3. (Color online) $V(z)$ for the QW structure of Fig. 2 with doping densities $n_{Dl}=3.0\times10^{11}$ cm^{-2} and $n_{Dr}=2.4\times10^{11}$ cm^{-2}. The inset shows $V(z)$, E_F, the energy eigenvalues, and $N_{\rm el}(z)$ in the well region. Resulting electron densities: $n_{\rm el}=1.24$, $n_{Sl}=1.75$, and $n_{Sr}=2.41$, all in 10^{11} cm^{-2}.

$z=d_l$ heavily overlap. Then the electrons are no longer bound to individual donors, but they are bound to the translation-invariant states (a subband) in the potential minimum produced by the positively charged plane, which we use to describe the electrostatic effects of the donors. If, however, the donor density n_{Dl} is so small, that individual shallow donor states survive, such states will not be ionized, if their energy $E_{\rm sd}<V(d_l)$ falls below the Fermi energy. Self-consistency will require a thermal equilibrium situation in which $E_{\rm sd}-E_F\sim k_BT$ so that only a part of the donors will be ionized, and hopping conduction between donor states becomes possible. We have also analyzed this case and found qualitatively similar results to those presented in the following, although for the case of nonoverlapping donor states the typical heavy-doping saturation behavior sets in at a lower doping level n_{Dl} (since $E_{\rm sd}<E_1^{\rm pc}$).

In the following, we will consider the case of overlapping donor states which leads to band—instead of hopping—conduction in the PC, and we treat the electron density in this band just as that in the desired 2DES. We will consider only situations with sufficiently thick spacer so that the low-energy eigenfunctions in the QW and those in the PC at d_l have practically no overlap. Therefore, for a given potential $V(z)$, we will calculate the eigenfunctions $\psi_n^{\rm qw}(z)$ and eigenenergies $E_n^{\rm qw}$ for the quantum well in a sufficiently thick layer containing the QW, and the eigenfunctions $\psi_n^{\rm pc}(z)$ and eigenenergies $E_n^{\rm pc}$ for the PC in a corresponding layer, containing the PC and having no overlap with the other layer. Thus, we get in addition to the electron density $N_{\rm el}^{\rm qw}$ in the QW, Eq. (9), the electron density

$$N_{\rm el}^{\rm pc}(z)=D_x\sum_n|\psi_n^{\rm pc}(z)|^2(E_F-E_n^{\rm pc})\,\theta(E_F-E_n^{\rm pc}),\qquad(11)$$

in the PC, with the DOS $D_x=D_0m^\star(x)/m^\star(0)$ in $Al_xGa_{1-x}As$. Integrating this over z, we get the area density of electrons in the PC,

$$n_{\rm el}^{\rm pc}=D_x\sum_n(E_F-E_n^{\rm pc})\,\theta(E_F-E_n^{\rm pc}).\qquad(12)$$

To calculate the Hartree potential $V_H(z)$, we have to replace $N_{\rm el}(z)$ in Poisson's Eq. (7) by the total density $N_{\rm mob}(z)=N_{\rm el}^{\rm qw}(z)+N_{\rm el}^{\rm pc}(z)$ of mobile electrons.

To solve the self-consistency problem, we first choose a value

$$n_{\rm mob}=n_{\rm el}^{\rm qw}+n_{\rm el}^{\rm pc}\qquad(13)$$

for the total area density of mobile charges. To determine the surface charges, we replace in Eq. (6) $n_{\rm el}$ by $n_{\rm mob}$ and estimate an approximate value for $V_H(s_r)$. For this we make a reasonable choice of $n_{\rm el}^{\rm qw}$ (resulting in $n_{\rm el}^{\rm pc}=n_{\rm mob}-n_{\rm el}^{\rm qw}$) and an ansatz for the z dependence of $N_{\rm el}^{\rm qw}(z)$ and $N_{\rm el}^{\rm pc}(z)$ that allows to calculate the corresponding $V_H(z)$ from Poisson's equation. For example, we may neglect the thicknesses of the mobile charge layers, $N_{\rm el}^{\rm qw}(z)=n_{\rm el}^{\rm qw}\delta(z-w_0)$ and $N_{\rm el}^{\rm pc}(z)=n_{\rm el}^{\rm pc}\delta(z-d_l)$, which leads, with the notation introduced below Eq. (6), to the approximation

$$D_SV_H(s_r)-n_{\rm mob}=-g_{srw0}n_{\rm el}^{\rm qw}-g_{srdl}n_{\rm el}^{\rm pc}.\qquad(14)$$

With this we calculate n_{Sl} from Eq. (6), which together with n_{Dl} yields the potential $V_{\rm fc}(z)$ in the region of mobile charges. With this and the starting value of $V_H(z)$ we solve the eigenvalue problems for QW and PC. Two cases are possible. First, if the lowest eigenvalues satisfy $E_1^{\rm cp}>E_1^{\rm qw}$, we try for the Fermi energy of the mobile charges $E_F^{\rm mob}=E_1^{\rm qw}+n_{\rm mob}/D_0$. If $E_F^{\rm mob}\le E_1^{\rm cp}$, we take this value and $n_{\rm el}^{\rm pc}=0$. If $E_F^{\rm mob}>E_1^{\rm cp}$, we assume that in both the QW and the PC only the lowest subbands are occupied, and get from Eqs. (10), (12), and (13)

$$E_F^{\rm mob}=[n_{\rm mob}+D_0E_1^{\rm qw}+D_xE_1^{\rm cp}]/(D_0+D_x).\qquad(15)$$

In the second case, $E_1^{\rm cp}\le E_1^{\rm qw}$, we try $E_F^{\rm mob}=E_1^{\rm pc}+n_{\rm mob}/D_x$. If $E_F^{\rm mob}\le E_1^{\rm qw}$, we take this value and $n_{\rm el}^{\rm qw}=0$, if not, we take $E_F^{\rm mob}$ from Eq. (15).

With $E_F=E_F^{\rm mob}$ we calculate from Eqs. (9)–(12) a new electron density $N_{\rm mob}(z)$ and a new $V_H(z)$. Using weighted iteration, we iterate with fixed $V_{\rm fc}(z)$ to convergence.

Taking the converged $V_H(z)$ and inserting $V_H(s_r)$ into Eq. (6), we find new n_{Sl} and $V_{\rm fc}(z)$, for which we again perform the self-consistency calculation of $N_{\rm mob}(z)$ and $V_H(z)$. With the converged solution we calculate $V_{\rm fc}(z)$ and a new n_{Sl}, until these have sufficiently stable values. In this situation we get for the chosen value of $n_{\rm mob}$ a Fermi energy $E_F^{\rm mob}$ for the mobile electrons in QW and PC, and a surface Fermi energy $E_F^S=n_{Sl}/D_S$. Now we vary the value $n_{\rm mob}$ until $E_F^{\rm mob}=E_F^S$ $(=E_F)$, and full consistency is obtained. The result of such a calculation is shown in Fig. 4.

We have calculated the electron distribution in the QW structure of Fig. 2 in all three doping regimes. The symbols in Fig. 5(a) show the results as functions of the doping level in the left doping sheet at $d_l=-75$ nm for fixed doping level $n_{Dr}=2.4\times10^{11}$ cm^{-2} in right doping sheet at $d_r=800$ nm. The lowest energy eigenvalues in the QW and the PC are indicated in Fig. 5(b). While they, together with the corresponding local potential minima, decrease rapidly with increasing n_{Dl} as long as they are larger than E_F, the decrease

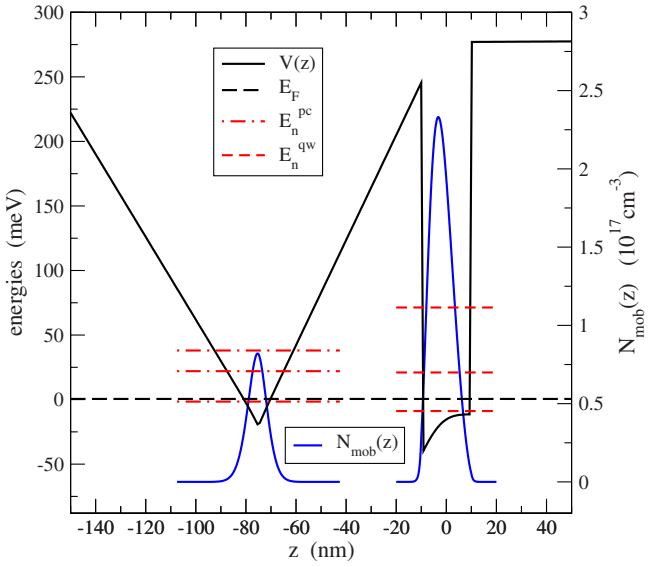

FIG. 4. (Color online) $V(z)$ for the structure of Fig. 2 in the region of PC and QW, for doping $\nu_{Dl}=5.5$ and $\nu_{Dr}=2.4$ (ν_μ means $n_\mu=\nu_\mu\times10^{11}$ cm^{-2}). Also shown are the Fermi energy E_F and, in the QW and the PC, the electron-density and the low-energy eigenvalues $E_n^{\rm qw}$ and $E_n^{\rm pc}$, respectively. Calculated electron densities: $\nu_{\rm el}^{\rm qw}=2.62$, $\nu_{Sl}=2.07$, $\nu_{Sr}=2.41$, and $\nu_{\rm el}^{\rm pc}=0.80$.

becomes much weaker, once the corresponding states are occupied. In the considered doping regime only the lowest subband in the quantum well and in the parallel channel can be partially occupied, as we anticipated above.

III. QUASICLASSICAL APPROXIMATION

If a 2DES in the quantum well and, eventually, in the parallel channel exists, the self-consistent calculation of the distribution of electrons between these 2D systems and the surface sheets becomes rather tedious. A rough estimate of this distribution can, however, be obtained by some crude semiclassical approximations. First, we neglect the thicknesses of the 2DESs,

$$N_{\rm el}^{\rm qm}(z)=n_{\rm el}^{\rm qm}\delta(z-w_0),\quad N_{\rm el}^{\rm pc}(z)=n_{\rm el}^{\rm pc}\delta(z-d_l). \tag{16}$$

Second, we take in Eqs. (10) and (12) only the lowest-energy state into account and replace its energy by

$$E_1^{\rm qm}\approx V(w_0)+E_{\rm bqw},\quad E_1^{\rm pc}\approx V(d_l)+E_{\rm bpc}, \tag{17}$$

respectively, with $E_{\rm bqw}\sim10$–15 meV and $E_{\rm bpc}\sim20$–30 meV. With these approximations, and for fixed values of $E_{\rm bqw}$ and $E_{\rm bpc}$, the position dependence of the potential $V(z)$ as well as the relations between the electron and the doping areal densities become in the zero-temperature limit piecewise linear.

For heavy doping we have, with $n_{Sl}=D_SE_F$,

$$n_{\rm el}^{\rm pc}=D_x[E_F-V(d_l)-E_{\rm bpc}]=(D_x/D_S)g_{dlsl}n_{Sl}-R_{\rm pc}, \tag{18}$$

where $R_{\rm pc}=D_x[E_c(0)+\Delta E_c(x_l)+E_{\rm bpc}]$ and, with the notation introduced below Eqs. (4) and (6), $g_{dlsl}=1+\gamma d_{dlsl}$, $d_{dlsl}=c_l-s_l+q_l(d_l-c_l)$. In addition we have

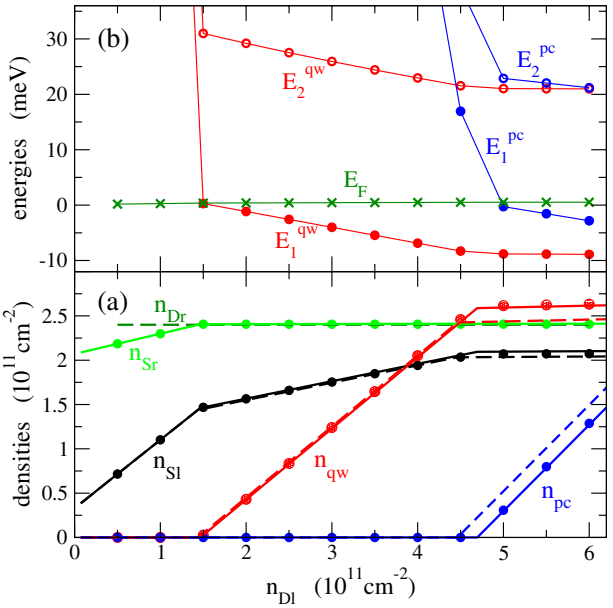

FIG. 5. (Color online) (a) Circles indicate the self-consistently calculated electron densities on surfaces (n_{Sl},n_{Sr}), in the QW ($n_{\rm qw}\equiv n_{\rm el}^{\rm qw}$), and in the PC ($n_{\rm pc}\equiv n_{\rm el}^{\rm pc}$) as function of n_{Dl} at fixed n_{Dr} (dashed horizontal line). (b) Fermi energy E_F and lowest energy eigenvalues in QW and PC obtained in the self-consistent calculation. The solid lines in (a) represent the quasiclassical approximation explained in Sec. III for $E_{\rm bqw}=10$ meV, $E_{\rm bpc}=30$ meV, the dashed lines for $E_{\rm bqw}=E_{\rm bpc}=0$.

$$\begin{aligned}n_{\rm el}^{\rm qw}&=D_0[E_F-V(w_0)-E_{\rm bqw}]\\&=(D_0/D_S)[g_{w0sl}n_{Sl}-\gamma d_{w0dl}(n_{Dl}-n_{\rm el}^{\rm pc})]-R_{\rm qw},\end{aligned} \tag{19}$$

with $R_{\rm qw}=D_0[E_c(0)+E_{\rm bqw}]$, $g_{w0sl}=1+\gamma d_{w0sl}$, $d_{w0dl}=q_l(w_l-d_l)+w_0-w_l$, and $d_{w0sl}=c_l-s_l+q_l(d_l-c_l)+d_{w0dl}$. Equation (2) now reads

$$n_{Sr}=g_{srsl}n_{Sl}-\gamma[d_{srdl}(n_{Dl}-n_{\rm el}^{\rm pc})-d_{srw0}n_{\rm el}^{\rm qw}+d_{srdr}n_{Dr}], \tag{20}$$

with $d_{srw0}=w_r-w_0+q_r(c_r-w_r)+s_r-c_r$, and the charge neutrality requires

$$n_{Sr}+n_{\rm el}^{\rm qw}+n_{\rm el}^{\rm pc}+n_{Sl}=n_{Dl}+n_{Dr}. \tag{21}$$

These two equations can be combined to

$$(1+g_{srsl})n_{Sl}=g_{srdl}n_{Dl}+g_{srdr}n_{Dr}-g_{srw0}n_{\rm el}^{\rm qw}-g_{srdl}n_{\rm el}^{\rm pc}. \tag{22}$$

Equations (18), (19), and (22) for the unknowns $n_{\rm el}^{\rm pc}$, $n_{\rm el}^{\rm qw}$, and n_{Sl} yield in the different doping regimes different linear dependences on n_{Dl}. In the weak-doping regime one has $n_{\rm el}^{\rm pc}=n_{\rm el}^{\rm qw}=0$, and Eq. (22) reduces to

$$n_{Sl}=(g_{srdl}n_{Dl}+g_{srdr}n_{Dr})/Z_0, \tag{23}$$

with $Z_0=1+g_{srsl}$ as discussed in Sec. II A.

In the intermediate-doping regime one has $n_{\rm el}^{\rm pc}=0$, and inserting Eq. (19) into Eq. (22) yields

$$n_{Sl} = [\alpha_1 n_{Dl} + g_{srdr} n_{Dr} + g_{srw0} R_{\rm qw}]/Z_1, \quad (24)$$

where $\alpha_1 = g_{srdl} + (D_0/D_S) g_{srw0} \gamma d_{w0dl}$ and $Z_1 = Z_0 + (D_0/D_S) g_{srw0} g_{w0sl}$. Inserting this into Eq. (19) yields

$$n_{\rm el}^{\rm qw} = \left[\frac{D_0}{D_S} (\beta_1 n_{Dl} + g_{w0sl} g_{srdr} n_{Dr}) - Z_0 R_{\rm qw} \right] \Big/ Z_1, \quad (25)$$

with $\beta_1 = g_{w0sl} g_{srdl} - \gamma d_{w0dl} Z_0 = g_{dlsl} g_{srw0}$. For $n_{\rm el}^{\rm qw} = 0$ this determines the critical doping

$$n_{Dl}^{cr1} = [(D_S/D_0) Z_0 R_{\rm qw} - g_{w0sl} g_{srdr} n_{Dr}]/\beta_1, \quad (26)$$

that separates the weak from the intermediate-doping regime.

For heavy doping one obtains

$$n_{Sl} = [\alpha_1 n_{Dl} + g_{srdr} n_{Dr} + g_{srw0} R_{\rm qw} + \alpha_1 R_{\rm pc}]/Z_2, \quad (27)$$

where $Z_2 = Z_1 + (D_x/D_S) \alpha_1 g_{dlsl}$. The critical doping level separating the intermediate-from the heavy-doping regime is

$$n_{Dl}^{cr2} = \left[\frac{Z_1 D_S R_{\rm pc}}{g_{dlsl} D_x} - g_{srw0} R_{\rm qw} - g_{srdr} n_{Dr} \right] \Big/ \alpha_1. \quad (28)$$

Inserting Eq. (27) into Eqs. (18) and (19) one obtains a result of the form

$$n_{\rm el}^{\rm qw} = \left[\frac{D_0}{D_S} \beta_1 n_{Dl} + \beta_2 n_{Dr} + \beta_3 R_{\rm qw} + \beta_4 R_{\rm pc} \right] \Big/ Z_2, \quad (29)$$

so that the slope of the function $n_{\rm el}^{\rm qw}(n_{Dl})$ in the heavy-doping regime is by a factor Z_1/Z_2 smaller than in the intermediate-doping regime.

For the model discussed so far, with Al-concentration $x_l = x_r = 0.3$, energy distance $E_c(0) - E_{\rm cnl} = 0.7$ eV, $E_{\rm bqw} = 10$ meV, and $E_{\rm bpc} = 30$ meV, one obtains $Z_1/Z_2 = 0.028$, $n_{Dl}^{cr1} = 1.467 \times 10^{11}$ cm^{-2} and $n_{Dl}^{cr2} = 4.694 \times 10^{11}$ cm^{-2}. The solid lines in Fig. 5(a) are calculated from Eq. (23) in the interval $0 < n_{Dl} < n_{Dl}^{cr1}$, from Eq. (24) in the interval $n_{Dl}^{cr1} < n_{Dl} < n_{Dl}^{cr2}$, and from Eq. (27) for $n_{Dl} > n_{Dl}^{cr2}$. For comparison, the dashed lines have been calculated with $E_{\rm bqw} = E_{\rm bpc} = 0$. Now the critical values $n_{Dl}^{cr1} = 1.439 \times 10^{11}$ cm^{-2} and $n_{Dl}^{cr2} = 4.464 \times 10^{11}$ cm^{-2} are somewhat smaller, since the potential minima reach the Fermi level at smaller values of n_{Dl}. This leads in the intermediate-doping region to slightly larger values of $n_{\rm el}^{\rm qw}$ and slightly smaller values of n_{Sl}, in the heavy-doping region to higher values of $n_{\rm el}^{\rm pc}$ and to smaller values of both $n_{\rm el}^{\rm qw}$ and n_{Sl}. A change of the right surface-electron density n_{Sr} is not visible on the scale of Fig. 5(a).

IV. SINGLE-INTERFACE HETEROSTRUCTURES

So far we have considered the formation of a 2DES in a quantum well structure with $Al_xGa_{1-x}As$ of the composition $x = x_l = x_r$ on both sides of the well. In the following we will consider the formation of a 2DES at a single interface, with $Al_xGa_{1-x}As$ of Al concentration $x = x_l > 0$ only to the left of the 2DES, and we put $x_r = 0$.

A. Strongly confined 2DES

Figure 6 shows an example of such a structure with δ-doping only on the left-hand side of the relevant interface.

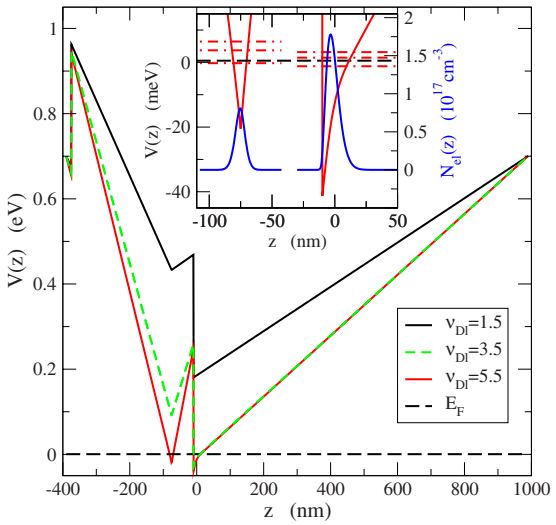

FIG. 6. (Color online) Effective conduction-band edges of a heterostructure with a $Al_{0.3}Ga_{0.7}As/GaAs$ interface at $z = -10$ nm and undoped GaAs in -10 nm $< z < 990$ nm for three doping strengths $n_{Dl} = \nu_{Dl} \times 10^{11}$ cm^{-2} in the plane $z = -75$ nm. The $Al_{0.3}Ga_{0.7}As$ layer is located in -375 nm $< z < -10$ nm, with a GaAs cap layer at -390 nm $< z < -375$ nm. The inset shows, for $\nu_{Dl} = 5.5$, the band-edge minima and the electron density $N_{\rm el}(z)$ at the interface and in the parallel channel.

The graphs represent the three different doping regions: (1) weak doping ($\nu_{Dl} = 1.5$), leading to surface charges but not to a 2DES inside the structure, (2) intermediate doping ($\nu_{Dl} = 3.5$) leading, in addition to the surface charges, to a 2DES near the interface, but no parallel channel, and (3) heavy doping ($\nu_{Dl} = 5.5$), leading in addition to surface charges and the desired 2DES to a parallel channel around the doping sheet, which suppresses the further increase of the electron density in the desired 2DES with further increasing doping. The inset of Fig. 6 visualizes some details of the latter case.

Figure 7(a) shows how the electron densities in the different parts of the structure change with doping. The solid symbols represent the results of self-consistent Hartree-type calculations. The corresponding lowest energy eigenvalues and the Fermi energy are given in Fig. 7(b). It is clearly seen that in the considered range of doping at most the lowest subbands in 2DESs at the interface and in the PC are occupied, if at all. The interpolating lines in Fig. 7(a) represent the quasi-classical approximation of Sec. III, with $E_{\rm bpc} = 30$ meV and $d_l = -75$ nm as approximation to energy eigenvalue and position of the PC and with $E_{\rm bif} = 10$ meV and $w_0 = 0$ nm as corresponding quantities of the 2DES at the interface. Whereas the result depends only weakly on the approximations $E_{\rm bif}$ and $E_{\rm bpc}$ of the lowest energy eigenvalues, it depends very sensitively on the value chosen for the position w_0 of 2DES near the interface.

The situation we have just considered is qualitatively similar to that of a quantum well. In both cases one needs a sufficiently strong doping to lower the potential minimum near quantum well or interface below the Fermi energy, so that the lowest bound state in this minimum can be occupied. The binding of the state is due to conduction-band discontinuities and, in the present case, due to an electrostatic field

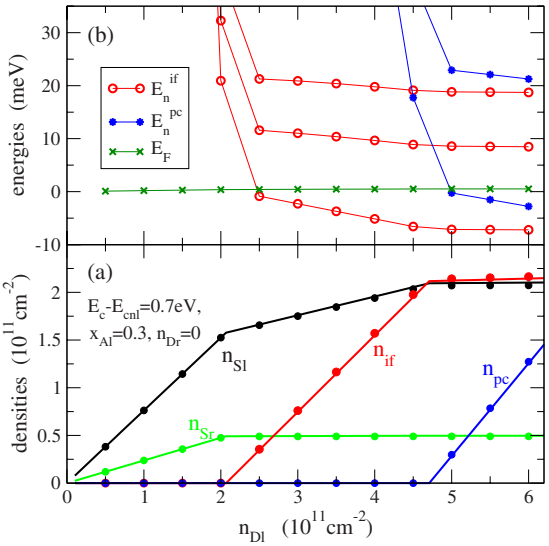

FIG. 7. (Color online) (a) Electron densities in surface states (n_{Sl} and n_{Sr}), in the 2DES near the interface (n_{if}) and in the parallel channel (n_{pc}) as functions of the doping density n_{Dl}, for n_{Dr}=0. Filled circles: self-consistent calculations; lines: quasiclassical approximation (see text). (b) Self-consistently calculated lowest energy eigenvalues E_n^{if} and E_n^{pc} in the potential minima near the IF and at the PC, respectively, and the Fermi energy.

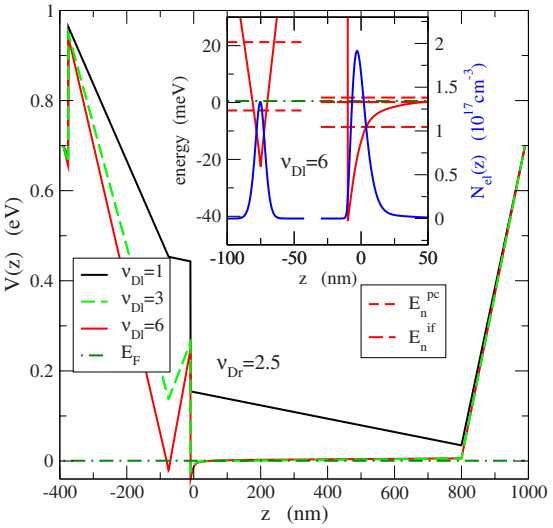

FIG. 8. (Color online) Effective conduction-band edges of a heterostructure as in Fig. 6, but with a δ doping of areal density $n_{Dr}=2.5\times10^{11}$ cm^{-2} at d_r=800 nm, for three doping strengths $n_{Dl}=\nu_{Dl}\times10^{11}$ cm^{-2} in the plane z=−75 nm. The inset shows, for ν_{Dl}=6, the band-edge minima and the electron density $N_{el}(z)$ at the interface and in the parallel channel. About 4% of the electrons in the 2DES at the interface occupy the second subband.

produced by remote charges, notably the right surface charge of density n_{Sr}. A qualitatively new situation occurs, if no such electrostatic field exists, and the 2DES is bound to the interface by its Coulomb attraction due to positive doping charges on the other side of the interface. Such situations may occur with samples on thick undoped GaAs substrates and buffer layers, where one has a potential drop similar to that in Fig. 6 at $z>0$, but extending over hundreds of μm, with a slope reduced by several orders of magnitude.

B. Weakly confined 2DES

We now consider a structure, where the reduction of the electrostatic field to the right of the interface is produced by a doping layer at d_r=800 nm, which essentially neutralizes the surface charge at $z=s_r$=990 nm. The interesting new effect is the occupation of the second subband in the "triangular" potential well at the interface, indicated in Fig. 8 by the fact, that two energy eigenvalues are lower than the Fermi energy, E_1^{if}=−8.586 meV, E_2^{if}=0.175 meV, E_3^{if}=1.753 meV, and E_F=0.518 meV. The population of the second subband with increasing doping on the left side starts already in the intermediate doping regime, long before the parallel channel at the left doping sheet occurs. Detailed investigation of the low-energy eigenstates shows that, for very small electron density in the 2DES at the interface, the effective "triangular" potential is determined by the weakly increasing linear term due to remote charges. This leads to a large extension of the lowest-energy wave function to the right of the interface, and a slow decrease in the curvature of the effective potential. With increasing n_{el}^{if} the potential dip at the interface becomes steeper, and the extension of the lowest-energy eigenfunction becomes smaller. Then the second-lowest eigenfunction, which has a much larger extension, is needed to allow for the smooth variation of the potential required by the self-consistency of electron distribution and Hartree potential. Figure 9 summarizes the results of the self-consistent calculation for various values of the doping strength.

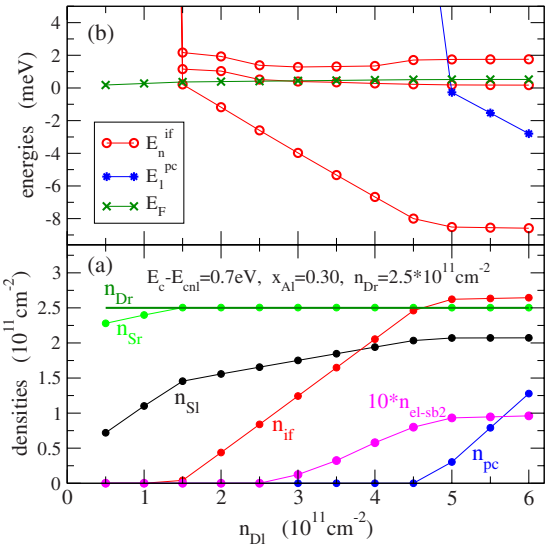

FIG. 9. (Color online) (a) Electron densities in surface states (n_{Sl} and n_{Sr}), in the 2DES near the IF (total n_{if} and in the second subband n_{el-sb2}), and in the PC (n_{pc}) as functions of the doping density n_{Dl}, for fixed n_{Dr}. Filled circles represent results of self-consistent calculations, lines are just guides to the eye. (b) Lowest energy eigenvalues E_n^{if} and E_n^{pc} in the potential minima near the IF and at the PC, respectively, and Fermi energy; $n_{el-sb2}>0$ if $E_2^{if}<E_F$.

V. DISCUSSION

A. Summary

The basic assumption of our approach is thermal equilibrium of the electrons in three types of possible states, the bound states near an interface or quantum well, which lead eventually to the desired 2DES, the bound states that may exist in the neighborhood of the doping layers, and the surface states. Depending on the strength of doping, three different regions are found. First, for weak doping one finds electrons in surface states but not in a 2DES inside the system. Second, for intermediate doping one finds, in addition to electrons in the surface states, a 2DES inside the sample with an areal density increasing linearly with the donor density. Finally, for strong doping a parallel channel occurs, which forms a parasitic 2DES located around the ionized donors and drastically suppresses the further increase of the electron density in the desired 2DES.

Quantitatively the distribution of electrons over the different parts of the heterostructure depends on material parameters, such as composition, thickness and position of the $Al_xGa_{1-x}As$ layers, and also on properties of the surface states, such as their DOS D_S and the energetic position of the charge neutrality level $E_{\rm cnl}$ with respect to the conduction band edge $E_c(0)$ of GaAs.

To be consistent with the frequently reported midgap pinning of the Fermi level in heterostructures with GaAs cap layers, we have taken $E_c(0)-E_{\rm cnl}=0.7$ eV. Changing this to the larger value $E_c(0)-E_{\rm cnl}=1.0$ eV suggested in the literature[8] results, at least for fixed $n_{Dr}=0$, in larger values for the critical doping values n_{Dl}^{cr1} and n_{Dl}^{cr2} which separate the different doping regimes. This leads to larger surface charges and to smaller electron densities in both the desired 2DES and the parallel channel.

If one fixes the surface related parameters and lowers the Al-concentration, i.e., the discontinuity of the conduction-band edge, one finds only minor changes in the weak- and intermediate doping region (due to minor changes of the dielectric constant of $Al_xGa_{1-x}As$), but the heavy doping region sets in at a lower n_{Dl}^{cr2}, resulting in smaller electron densities on the left surface and in the desired 2DES, but larger electron density in the parallel channel.

B. Parameter dependences

Quantitatively the density of the 2DES at the interface also depends strongly on geometrical parameters, such as the thickness of $Al_xGa_{1-x}As$ layer and the position of the doping layers, notably the spacer thickness. We give some examples based on the quasiclassical approximation of Sec. III, with fit parameters $E_{\rm bif}=10$ meV and $E_{\rm bpc}=30$ meV, as above.

In Fig. 10, we present results for single-interface heterostructures with an undoped GaAs buffer of 1 μm thickness, followed by an $Al_xGa_{1-x}As$ layer of thickness dAl and a 15 nm thick GaAs cap layer. We consider three values of dAl and keep the distance between the interface and the doped sheet in the $Al_xGa_{1-x}As$ layer fixed at 40 nm. For thinner $Al_xGa_{1-x}As$ layer, i.e., smaller distance between left surface and doping sheet, larger surface and doping charges are required to lower the effective conduction-band edge in the interface region so much, that a 2DES can occur at the interface. The same is true for the occurrence of a PC at the doping sheet.

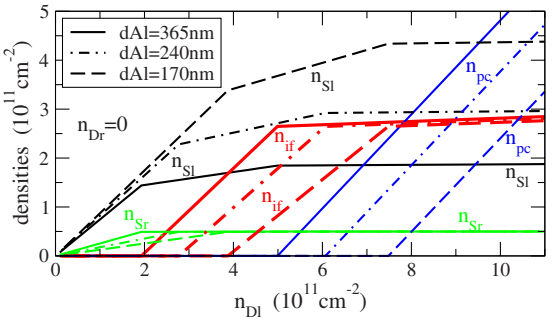

FIG. 10. (Color online) Electron densities in surface states (n_{Sl} and n_{Sr}), in the 2DES near the IF ($n_{\rm if}$), and in the PC ($n_{\rm pc}$) as functions of the doping density n_{Dl} of the left doping sheet in a single-interface heterostructure with undoped GaAs buffer of 1 μm thickness. $Al_xGa_{1-x}As$ layers (with $x=0.24$) of three different thicknesses dAl are considered, all with a 40 nm thick spacer.

In Fig. 11 we keep the thicknesses of the $Al_{0.24}Ga_{0.76}As$ layer, 365 nm, and of the GaAs buffer, 1 μm, fixed. In the lower part of the figure we consider an undoped buffer and three different positions of the doped sheet in the $Al_{0.24}Ga_{0.76}As$ layer, i.e., three different spacer thicknesses $sp=w_l-d_l$. As the spacer becomes thinner, the distance between doping charge and surface becomes larger. Thus it requires less charges to create a sufficiently large dipole po-

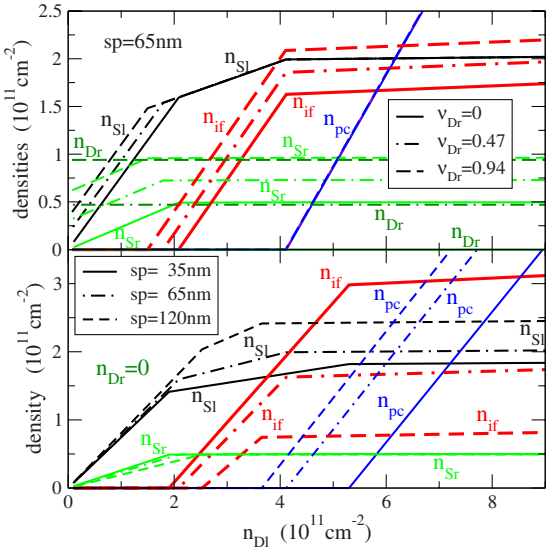

FIG. 11. (Color online) Electron densities on surfaces (n_{Sl} and n_{Sr}), of the 2DES near the IF ($n_{\rm if}$), and in the PC ($n_{\rm pc}$) as functions of the doping density n_{Dl} of the left doping sheet in a single-interface heterostructure. The GaAs buffer is 1 μm, the $Al_{0.24}Ga_{0.76}As$ layer is 365 nm and the following GaAs cap is 15 nm thick. Upper panel: fixed spacer thickness of 65 nm in the $Al_{0.24}Ga_{0.76}As$ and three doping densities $n_{Dr}=\nu_{Dr}\times 10^{11}$ cm^{-2} of the right doping sheet at 500 nm from the interface. Lower panel: undoped substrate, $n_{Dr}=0$, and three values of the spacer thickness in the $Al_{0.24}Ga_{0.76}As$.

TABLE I. Simple estimates of electron and ion densities according to Eqs. (30)–(33), for different values $E_c(0)$ and $\Delta E_c(x)$ (both measured in eV).

Case	$E_c(0)$	x	$\Delta E_c(x)$	$\nu_{\rm el}^{\rm if}$	$\tilde{\nu}_{Dl}$	ν_{Dr}	ν_{Sl}	ν_{Sr}
A	0.7	0.30	0.289	2.15	4.79	0	2.15	0.49
B	0.7	0.30	0.289	2.64	4.79	2.53	2.15	2.53
A	1.0	0.30	0.289	1.95	5.44	0	2.80	0.69
B	1.0	0.30	0.289	2.64	5.44	3.61	2.80	3.61
A	0.7	0.24	0.228	1.60	4.10	0	2.02	0.48
B	0.7	0.24	0.228	2.08	4.10	2.53	2.02	2.53

tential between surface and doping layer, to allow for the occurrence of a 2DES at the interface. As a consequence, for thinner spacer a 2DES occurs at lower doping level. To reach the heavy-doping limit, the potential at the doping sheet must be lowered below the Fermi energy, so that the potential difference between interface and doping sheet must be of the order of the conduction band discontinuity at the interface. Therefore, the critical electron density of the 2DES increases (nearly inversely proportional) with decreasing spacer thickness. As a consequence, the lower critical doping n_{Dl}^{cr1} decreases and the upper critical doping n_{Dl}^{cr2} increases, so that the intermediate-doping region increases with decreasing spacer thickness.

In the upper part of Fig. 11, we keep the spacer thickness 65 nm in the $Al_{0.24}Ga_{0.76}As$ layer fixed and consider additional doping of the buffer layer in a sheet 500 nm apart form the interface. We keep this doping so low that no parallel channel does occur near this doping sheet in the buffer. Increasing the doping level n_{Dr} in this sheet lowers the effective band-edge near the interface, so that the 2DES occurs at lower doping level n_{Dl} in the left sheet. Once a 2DES is present at the interface ($n_{\rm if}>0$), the right surface charge density n_{Sr} becomes nearly independent of the doping level n_{Dl} of the left doping sheet and the left surface charge density n_{Sl} becomes independent of the doping level n_{Dr} of the right doping sheet. In the heavy-doping regime both the left surface charge density n_{Sl} and the electron density $n_{\rm pc}$ of the parallel channel near d_l become independent of the doping level n_{Dr}. This type of screening effect was also found in the self-consistent calculations presented in Figs. 6 and 8. Since with increasing n_{Dr} the difference $n_{Sr}-n_{Dr}$ in the heavy-doping regime decreases, the saturation density $n_{\rm if}$ of the 2DES at the interface increases with increasing n_{Dr}.

C. Simple electrostatic estimates

While the quasiclassical approximation of Sec. III describes the doping dependence of the electron distribution over the different parts of the sample quite well in all three doping regimes, in the high-doping regime an even simpler electrostatic approximation is possible. For a rough estimate of the electron densities in the heavy doping regime one may neglect the binding energies in the desired 2DES and in the parallel channel since they are of the order of 10 meV and thus much smaller than $E_c(0)-E_{\rm cnl}$ and the conduction-band offset $\Delta E_c(x)$. We choose $E_{\rm cnl}=0$, neglect the x dependence of the dielectric constant, $\varepsilon(x)\approx\varepsilon(0)$, and discard quantum effects by putting $V(d_l)\approx V(w_0)\approx E_F\approx 0$. Then we can estimate the surface electron density $n_{Sl}=\nu_{Sl}\cdot 10^{11}$ cm^{-2} from the electrostatic dipole potential between s_l and d_l as

$$\nu_{Sl}\approx\eta\frac{[E_c(0)+\Delta E_c(x)]/\text{eV}}{[d_l-s_l]/\text{nm}}, \tag{30}$$

where $\eta=([4\pi e^2/\varepsilon(0)]\times 10^4/[\text{eV cm}])^{-1}=685.4$. To proceed we distinguish the cases of (A) strongly confined 2DES (Sec. IV A) and of (B) weakly confined 2DES (Sec. IV B).

For case (A) we have no doping on the right side, $n_{Dr}=0$. This yields

$$\nu_{Sr}\approx\eta\frac{E_c(0)/\text{eV}}{[s_r-w_0]/\text{nm}}, \tag{31}$$

and, since the electric field in $d_l<z<w_0$ is proportional to $n_{\rm el}^{\rm if}+n_{Sr}$,

$$\nu_{\rm el}^{\rm if}+\nu_{Sr}\approx\eta\frac{\Delta E_c(x)/\text{eV}}{[w_0-d_l]/\text{nm}}. \tag{32}$$

From Eqs. (30)–(32) one easily obtains $\nu_{\rm el}^{\rm if}$ and $\tilde{\nu}_{Dl}\equiv\nu_{Dl}-\nu_{\rm el}^{\rm pc}=\nu_{Sl}+\nu_{\rm el}^{\rm if}+\nu_{Sr}$.

For case (B) we assume that doping and surface charge on the right side cancel, $\nu_{Sr}=\nu_{Dr}$, so that $V(d_r)=0$ and

$$\nu_{Dr}\approx\eta\frac{E_c(0)/\text{eV}}{[s_r-d_r]/\text{nm}},\quad \nu_{\rm el}^{\rm if}\approx\eta\frac{\Delta E_c(x)/\text{eV}}{[w_0-d_l]/\text{nm}}. \tag{33}$$

Equations (32) and (33) show that the upper limit for the electron density in the desired 2DES is proportional to the conduction-band offset $\Delta E_c(x)$ at the interface, and inversely proportional to the spacer thickness $w_l-d_l\lesssim w_0-d_l$. The same is true for case (A), if the substrate thickness $s_r-w_l\gtrsim s_r-w_0$ is very large, so that, according to Eq. (31), the surface electron density n_{Sr} is very small. Some numerical results for the heterostructure discussed so far are given in Table I.

D. Modifications of the model

For the cases considered here, the heavy-doping regime corresponds to $n_{Dl}>4\times 10^{11}$ cm^{-2}. Since the radius of a shallow donor state is of the order of an effective Bohr radius $a_B^\star\sim 10$ nm, such a state covers an area of about $\pi(a_B^\star)^2\sim 3\times 10^{-12}$ cm^2, and in the heavy-doping regime these

states overlap. Thus it is reasonable to assume band conduction rather than hopping conduction in the PC, of course with a low mobility, since the electron states are centered in the plane of ionized donors. If, on the other hand, the parallel channel would occur at a considerable lower area density n_{Dl} of shallow donor states, the electrons of the PC would have to occupy localized states, and Coulomb correlation effects might become important.[9] Neglecting such effects, we have simulated such a situation by assuming that homogeneously distributed shallow donor states of areal density n_{Dl} are partially occupied according to the Fermi-Dirac distribution at the relevant low temperature. The areal electron density in these states is then the electron density $n_{\mathrm{el}}^{\mathrm{pc}}$ of the PC. This model leads to very similar results, but the PC occurs at a slightly lower doping level n_{Dl}, since now the shallow-donor energy below the effective conduction-band edge must be compared with the Fermi energy and not the (higher) ground-state energy in the potential well formed by the effective conduction-band-edge minimum near the doping sheet.

In the simple electrostatic estimate the value $\tilde{\nu}_{Dl} \cdot 10^{11}\ \mathrm{cm}^{-2} = n_{Dl} - n_{\mathrm{el}}^{\mathrm{pc}}$ coincides with the critical doping n_{Dl}^{cr2}, which separates the intermediate-from the heavy-doping regime. Further increase of n_{Dl} just increases $n_{\mathrm{el}}^{\mathrm{pc}}$, so that the difference remains constant. In the quasiclassical approximation of Sec. III, on the other hand, the potential and, as a consequence, the electron densities in the 2DES and the left surface increase linearly with increasing n_{Dl}, although the slope of this increase in the heavy-doping region is much smaller than in the intermediate-doping region. In the self-consistent quantum calculation the shape of the confinements potentials near the interface and in the parallel channel changes with increasing doping, so that slight deviations from the linear dependences result. Quantum phenomena such as the occupation of a higher subband, as discussed in Sec. IV B, require of course a fully self-consistent treatment. To get reliable experimental information about the occupation of a higher subband or a PC is difficult, but possible if the desired 2DES exhibits the quantized Hall effect.[10]

For the sake of completeness, we have also investigated the dependence of the results on the surface DOS D_S. We found that the charge distribution in the structure remains essentially unchanged, if we reduce the value of D_S by a factor of ten. The main change is that E_F increases by a factor of ten (from about 0.5 meV to about 5 meV), and that, as a consequence of the self-consistency, the potential in the neighborhood of interface and left doping layer increases by about the same amount, so that the densities remain nearly unchanged.

We have also relaxed the requirement of thermodynamic equilibrium. Starting from an equilibrium situation in the intermediate-doping regime, we fixed the surface charges and the doping level in the right doping sheet, and required for increasing doping of the left sheet only equilibrium of electrons in the center region including the neighborhood of interface (or quantum well) and parallel channel, without coupling to the surface electrons. Then the increase of the function $n_{\mathrm{el}}^{\mathrm{if}}(n_{Dl})$ is somewhat steeper than in total equilibrium, and the saturation in the heavy-doping regime is reached at a slightly smaller doping than n_{Dl}^{cr2}. But in the heavy-doping regime we find essentially the same electron distribution as in the total equilibrium, only the Fermi energy of the center region is higher than that of the surface electrons. This difference is, however, nearly compensated by a corresponding change of the self-consistent potential.

ACKNOWLEDGMENTS

Stimulating discussions with S. Schmult, W. Dietsche, and K. von Klitzing are gratefully acknowledged.

[1] H. L. Stormer, R. Dingle, A. C. Gossard, and W. Wiegmann, Inst. Conf. Ser. London **43**, 557 (1978).
[2] R. Dingle, H. L. Stormer, A. C. Gossard, and W. Wiegmann, Appl. Phys. Lett. **33**, 665 (1978).
[3] N. Read, Physica B **298**, 121 (2001).
[4] M. Dolev, M. Heiblum, V. Umansky, A. Stern, and D. Mahalu, Nature (London) **452**, 829 (2008).
[5] C. Siegert, A. Ghosh, M. Pepper, I. Farrer, and D. A. Ritchie, Nat. Phys. **3**, 315 (2007).
[6] E. H. Hwang and S. Das Sarma, Phys. Rev. B **77**, 235437 (2008).
[7] S. G. Louie, J. R. Chelikovsky, and M. L. Cohen, J. Vac. Sci. Technol. **13**, 790 (1976).
[8] W. Mönch, *Semiconductor Surfaces and Interfaces*, Springer Series in Surface Sciences Vol. 26 (Springer-Verlag, Berlin, 2001).
[9] A. L. Efros, F. G. Pikus, and G. G. Samsonidze, Phys. Rev. B **41**, 8295 (1990).
[10] M. Grayson and F. Fischer, J. Appl. Phys. **98**, 013709 (2005).
[11] E. F. Schubert and K. Ploog, Phys. Rev. B **30**, 7021 (1984).
[12] *Semiconductors*, edited by O. Madelung, Landolt-Börnstein, New Series, Group III, Vol. 17a (Springer, Berlin, Heidelberg, 1982).
[13] J. Menéndez, A. Pinczuk, D. J. Werder, A. C. Gossard, and J. H. English, Phys. Rev. B **33**, 8863 (1986).
[14] R. Winkler, *Spin-Orbit Coupling Effects in Two-dimensional Electron and Hole Systems*, Springer Tracts in Modern Physics Vol. 191 (Springer-Verlag, Berlin, Heidelberg, New York, 2003).